ELSEVIER

Polymer 43 (2002) 123–129

polymer

www.elsevier.com/locate/polymer

Temperature-dependent property development in hydrogels derived from hydroxypropylcellulose

Samuel G. Hirsch, Richard J. Spontak*

Departments of Materials Science and Engineering and Chemical Engineering, North Carolina State University, Raleigh, NC 27695, USA

Received 22 June 2001; received in revised form 20 August 2001; accepted 27 August 2001

Abstract

Hydrogels constitute an important class of responsive materials that are employed in numerous biomedical and personal-care applications, most notably of which are controlled drug delivery, separations and superabsorbency. Since aqueous hydroxypropylcellulose (HPC) solutions exhibit lower critical solution behavior, hydrogels produced from this cellulose ether are temperature-responsive, swelling at low temperatures and contracting at high temperatures. If HPC hydrogels are synthesized at temperatures in the single-phase regime, they remain nonporous, whereas those crosslinked in the biphasic regime become microporous. In this work, we employ the modified temperature-induced phase separation (TIPS) protocol to generate nonporous and microporous HPC hydrogels crosslinked at different temperatures. The dynamic mechanical properties and swelling capacities of these hydrogels are reported as functions of crosslinking temperature.

Keywords: Hydrogels; Hydroxypropylcellulose; Temperature-induced phase separation

1. Introduction

Hydroxypropylcellulose (HPC) is one of the most important chemical derivatives of cellulose due to its considerable hydrophilicity, complex phase behavior and ease of production [1–5]. At relatively low polymer concentrations and ambient temperature conditions, aqueous HPC forms an isotropic solution phase. As the concentration of HPC is increased, the semi-rigid HPC molecules order into a cholesteric mesophase. Conversely, since aqueous HPC exhibits lower critical solution temperature (LCST) behavior, an increase in temperature under isoplethic conditions induces turbidity and the onset of phase separation (at a composition-dependent cloud point, T_c), resulting in HPC-rich and -lean phases. Due to their tremendous hydrophilicity, cellulose ethers such as HPC are ideally suited for hydrogel fabrication [6–8]. By chemically crosslinking low-viscosity isotropic solutions of aqueous HPC, a macromolecular network possessing the physical and chemical properties of HPC can be readily generated. The resultant hydrogel is temperature-responsive, swelling in the presence of water at temperatures below T_c and contracting at temperatures above T_c [9,10]. Such HPC hydrogels are of current technological relevance in various drug delivery, separation and superabsorbency applications [11–14]. Hydrogels prepared from isotropic HPC solutions consist of a spatially homogeneous network and appear nonporous, as evidenced by the field-emission scanning electron microscopy (FESEM) image displayed in Fig. 1(a). Using methods described earlier [15,16] we have rapidly vitrified (by plunging into liquid ethane cooled by liquid nitrogen) and subsequently freeze-dried the 9 wt% HPC hydrogel examined in this figure (crosslinked at ca. 24°C, which is below the T_c of 44°C) prior to Au/Pd coating and FESEM analysis at an accelerating voltage of 5 kV.

Crosslinking the same HPC solution for 5 min at a temperature of 49°C (above T_c), followed by 24 h at ambient temperature, according to the modified temperature-induced phase separation (TIPS) protocol of Gehrke and co-workers [15] yields the microporous hydrogel presented in Fig. 1(b). In this hydrogel, discrete pores measuring between 3 and 5 μm in diameter are separated by HPC struts typically measuring 1–3 μm across. Due to their heterogeneous morphology, microporous hydrogels are more rapidly responsive to environmental stimuli and facilitate uptake/expulsion of dissolved compounds [17,18]. An interesting feature of the microporous HPC hydrogel in Fig. 1(b) is the surface modulation evident along the HPC struts. Examination of the same hydrogel, tagged with a cellulose-selective

* Corresponding author. Tel.: +1-919-515-4200; fax: +1-919-515-7724.
E-mail address: rich_spontak@ncsu.edu (R.J. Spontak).

0032-3861/02/$ - see front matter
PII: S0032-3861(01)00608-5

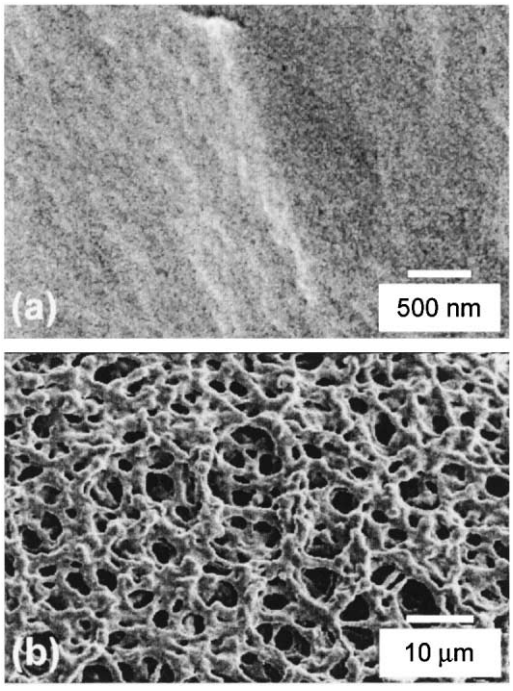

Fig. 1. Field-emission scanning electron micrographs of freeze-dried [15,16] HPC hydrogels crosslinked for (a) 24 h at 24°C (nonporous) and (b) 5 min at 49°C, followed by 24 h at 24°C (microporous). The HPC concentration of each solution is 9 wt%, and images have been acquired with a JEOL-6400 microscope operated at 5.0 kV.

fluorescent dye (Calcofluor White), by confocal laser scanning microscopy (CLSM) yields the optical sections shown in Fig. 2. The sections displayed in Fig. 2(a) demonstrate how the hydrogel morphology in its hydrated state varies as a function of specimen depth, whereas the single section in Fig. 2(b) provides a more global view of the hydrated hydrogel morphology. Fig. 3 provides a magnification-matched comparison of a three-dimensional CLSM reconstruction (Fig. 3(a)) and a topological FESEM image (Fig. 3(b)) to demonstrate the similarities and differences in hydrogel morphology.

Small nodules measuring ca. 2 μm in diameter along the HPC struts in the CLSM images (Figs. 2 and 3) are presumed to be responsible for the strut modulation visible in the FESEM images and appear qualitatively similar to those observed [19] by CLSM in other noncellulosic hydrogels. Existence of nodules is consistent with recent findings by Gao et al. [20], who propose that the mechanism of phase separation in (dilute) aqueous HPC solutions involves the formation of discrete HPC microspheres. According to their light scattering measurements, the diameters of these particles (at a constant HPC composition of 5.15×10^{-5} g/cm^3) increase in size from 0.18 μm at 40°C to 0.55 μm at 45°C. Gao et al. [20] also report that these particles increase in size with increasing HPC concentration. On the basis of these observations, we expect that such particles, if they form, should measure on the same size scale as the nodules evident in the CLSM images shown here at the present conditions of solution concentration and crosslinking temperature. Moreover, it follows that, if aqueous HPC phase separation at temperatures in excess of T_c initiates by the formation of discrete particles, such particles would tend to aggregate as the solution concentration is increased. This anticipated feature is also seen in Figs. 2 and 3.

We provide our microscopy results (Figs. 1–3) here, rather than in subsequent sections, for illustrative purposes (experimental details are included in the figure captions) so that the effect of crosslink temperature on gel morphology

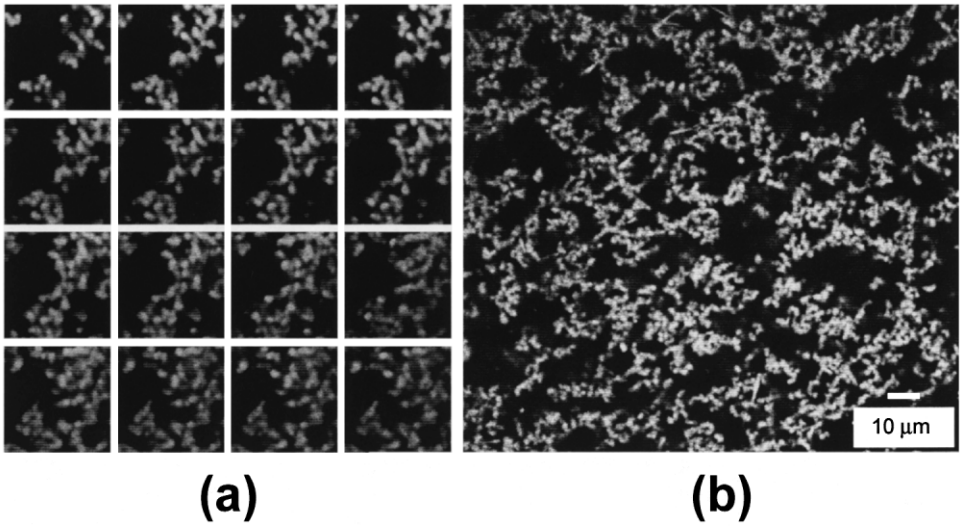

Fig. 2. Optical sections collected by CLSM (100× oil-immersion lens) from the HPC hydrogel displayed in Fig. 1(b) and tagged with a cellulose-selective fluorescent dye (Calcofluor White) while hydrated. A UV laser ($\lambda = 350$ nm) has been used to excite the dye during image acquisition with an inverted Leica SP DM-IRB microscope. In (a), a sampling of every fifth x–y section is shown as a function of specimen depth along the z-axis (arranged from left to right and top to bottom). Each image represents an average of 4 or 8 scans and corresponds to a specimen thickness of approximately 0.1 μm. A larger view of one section, collected with a 63× water-immersion lens, is shown for completeness in (b).

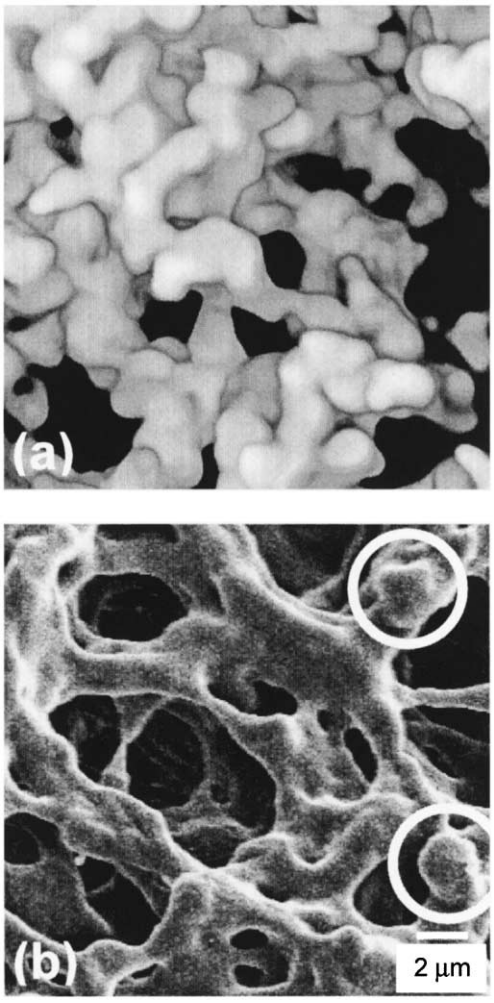

Fig. 3. Comparison of the microporous HPC hydrogel morphology as revealed by a volumetrically reconstructed CLSM image in (a) and a FESEM image in (b). Recall that the specimen in (a) is fully hydrated, whereas the one displayed in (b) has been freeze-dried. Circled regions in (b) identify nodular features that are also visible in (a). The reconstruction has been generated with image oversampling and interpolation enhancements in T3D Plot after noise reduction and gamma correction in Adobe Photoshop.

can be immediately appreciated. According to the modified TIPS protocol [15], adjustable synthesis variables include (i) the initial temperature below T_c and the crosslink time (t_b) at this temperature, (ii) the temperature above T_c and the corresponding crosslink time (t_x) and (iii) the final temperature below T_c and the crosslink time (t_a) at this temperature. In this work, we have synthesized one series of microporous HPC hydrogels at temperatures above T_c (all with $t_b = 2.5$ min and most with $t_x = 5.0$ min and $t_a = 24$ h), as well as a companion series of nonporous HPC hydrogels crosslinked for 24 h at sub-ambient temperatures. The dynamic mechanical responses and swelling capacities of the hydrogels in these two series are compared to ascertain, in systematic fashion, the effect of hydrogel morphology on bulk properties.

2. Experimental

2.1. Materials

The HPC employed in this study was obtained in powder form from the Aldrich Chemical Co. (Milwaukee, WI, USA) and used as-received. Its molecular weight was 100 kg/mol, and its molar substitution (according to the manufacturer) was between 3.4 and 4.4. Divinyl sulfone (DVS, 97% pure), the crosslinking agent, and reagent-grade sodium hydroxide (NaOH), the crosslinking reaction catalyst, were also purchased from Aldrich.

2.2. Methods

Master batches of 14 wt% HPC solution were prepared by dissolving HPC powder in distilled water at ambient temperature for 72 h. Small portions (2.0 g each) of these batches were removed to individual beakers and, upon adding 5 M NaOH (50 μl), slowly stirred to ensure uniform mixing while avoiding bubble formation. Initial addition of NaOH by micropipette resulted in the formation of minute white speckles. Disappearance of these speckles (after about 2 min of agitation) signaled complete dissolution of NaOH, after which time DVS (50 μl) was added. Each solution was mixed thoroughly for 75 s and then poured into a mold, which consisted of two 120 mm × 160 mm × 5.0 mm glass plates separated by a silicon gasket measuring about 1.6 mm thick. Once the solution spread evenly within the confines of the gasket on one plate, the second glass plate was carefully laid on top (starting from one edge) to complete the mold, which was held in place by spring clips. The solutions were crosslinked at temperatures (in 5°C increments) above and below ambient temperature, as well as above and below T_c (=39–40°C, according to spectrophotometry), to determine the effect of crosslinking temperature, as well as morphology, on hydrogel properties.

For hydrogels crosslinked at elevated temperatures, the mold was immersed for 5.0 min (unless otherwise stated) in a water bath preheated to a specific temperature at which DVS crosslinking occurred. (The time from the addition of DVS to immersion of a filled mold in the water bath was 2.5 min.) After 5.0 min at an elevated temperature, the mold was immediately removed from the bath, and the solution was allowed to cool and continue crosslinking for 24 h at ambient temperature in a second water bath. Note that HPC solutions were also crosslinked at sub-ambient temperatures, as well as at a few discrete temperatures above ambient, for 24 h. Upon termination of crosslinking, the resultant materials were removed from their molds and subsequently placed into distilled water baths at ambient temperature to extract excess (uncrosslinked) DVS. The water was changed every 24 h over a period of three days, after which time the crosslinked materials were stored in distilled water at ambient temperature prior to analysis. Biphasic solutions crosslinked at temperatures above T_c appeared turbid, confirming

that they were phase-separated. At 59 and 64°C, the materials contracted and pulled away from the gasket on each side of the mold by about 2 and 4 mm, respectively.

A Rheometrics dynamic stress rheometer (DSR) equipped with 25 mm platens was operated in parallel-plate geometry to measure the dynamic rheological properties of the crosslinked HPC systems. Specimen wafers measuring 25 mm in diameter were cut from the crosslinked materials with a home-made stamping tool. To avoid specimen slippage during analysis, 400 fine grit sandpaper was cut to shape and attached to both platens with double-sided tape. Dynamic stress (τ) sweeps were performed from 10–50 dyn/cm^2 to the point at which the material failed at a frequency (ω) of 1.0 rad/s to ascertain the linear viscoelastic (LVE) limit. In this limit, the dynamic storage (G') and loss (G'') moduli are unaffected by the applied load and are independent of τ. From these results, stress amplitudes were selected for the acquisition of ω spectra in the LVE regime at ambient temperature. Swelling capacity tests were conducted with samples cut into arbitrary shapes, as well as into the wafers described above. Freshly cut samples were dried in air at ambient temperature for 24 h and then rehydrated in distilled water for 48 h. After the fully swollen samples were weighed, they were kept in an active fume-hood for 24 h and then dried under vacuum in an oven maintained at 61°C for an additional 24 h and subsequently reweighed. This cycle was repeated in sets of 2 for up to 5 cycles before samples were replaced.

3. Results and discussion

Fig. 4 shows the ω spectra collected from two aqueous HPC solutions crosslinked for 24 h at sub-ambient temperatures (5 and 14°C). Under these conditions, the solutions remain completely homogeneous. According to the data presented in this figure, G' (and to a lesser extent, G'') exhibits little, if any, dependence on ω. Another important feature of these data is that G' exceeds G'' by more than an order of magnitude over the entire ω range explored. Taken together, these two characteristics — G' independent of ω and $G' > G''$ — confirm that these two crosslinked materials behave as gels [21,22] Indeed, this behavior is observed with regard to all the materials produced during the course of this study. While the data in Fig. 4 suggest that the HPC hydrogel crosslinked at 5°C exhibits higher moduli than the one crosslinked at 14°C, this apparent difference is found to be an artifact of the hydrogel synthesis. Representative values of G' measured from specimens obtained from different positions (middle, outer middle and outer center) of the large hydrogel sheets prepared at sub-ambient temperatures are presented in Fig. 5, and reveal that crosslinking effectiveness is not homogeneous, appearing to decrease radially with decreasing temperature. Such heterogeneous crosslinking is attributed to temperature-induced changes in crosslink reaction kinetics, an increase in solution viscosity or (most likely) a combination of both. If such variation can be precisely regulated to generate a two-dimensional gradient in crosslink efficacy, it may prove useful in (i) the production of multifunctional HPC hydrogels or (ii) the analysis of such hydrogels via combinatorial methods. Mean modulus values derived from all the data corresponding to this series of HPC hydrogels are found to be relatively insensitive to temperature.

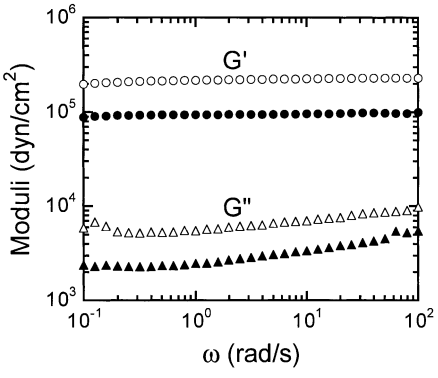

Fig. 4. Frequency (ω) spectra of the dynamic elastic (G', circles) and viscous (G'', triangles) moduli for 14 wt% HPC hydrogels ($t_x = 24$ h) at 5°C (open) and 14°C (filled). In both cases, the moduli are ω-independent and G' clearly exceeds G'' by more than an order of magnitude, which together confirm that these materials exhibit gel behavior [21,22].

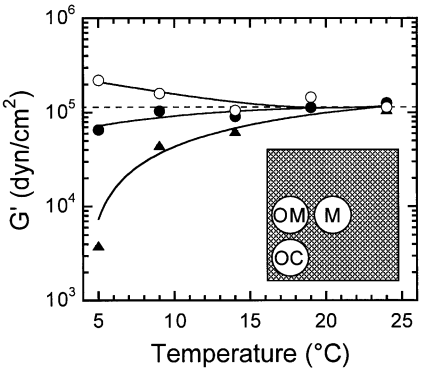

Fig. 5. Representative G' measured from 14 wt% HPC hydrogels ($t_x = 24$ h) at the middle (M, ○), outside middle (OM, ●) and outside corner (OC, ▲) of the specimen sheets as a function of crosslink temperature. A schematic diagram showing these positions is provided in the inset. The solid lines are guides for the eye, whereas the dashed line identifies the mean of all the data collected from hydrogels prepared at sub-ambient temperatures.

The dependence of G' on ω is displayed in Fig. 6 for several HPC hydrogels crosslinked for 5.0 min at ambient temperature and above. Hydrogels prepared at temperatures up to 54°C exhibit similar ω spectra as those prepared at sub-ambient temperatures. Note, however, that the hydrogels crosslinked at 59 and 64°C differ slightly in that they show evidence of network collapse at high ω. Since the existence of a network is established at low ω, failure at high ω most likely reflects thin or defective HPC struts comprising the microporous hydrogel morphology. At sufficiently high ω, these features may weaken or break apart

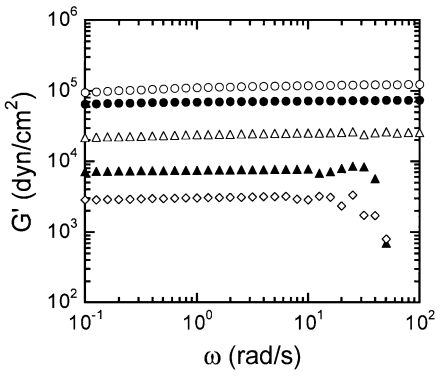

Fig. 6. Variation of G' with respect to ω for 14 wt% HPC hydrogels ($t_x = 5.0$ min) at several different temperatures (in °C) — 24 (○), 39 (●), 54 (Δ), 59 (▲) and 64 (◇) — prior to crosslinking for 24 h at 24°C. Two of the microporous hydrogels exhibit signs of structural alteration at high ω.

altogether, in which case the network required to endow the material with solid-like character likewise falters. The end result is that G' plummets, as seen in this figure. Values of G' derived from ω spectra such as the ones provided in Fig. 6 are shown as a function of crosslink temperature in Fig. 7. Since the minor variation evident in G' at temperatures below T_c is within the accepted level of accuracy (±15%) for rheological measurements, G' can be considered independent of temperature under these conditions. This result agrees with the temperature dependence of G' for HPC hydrogels crosslinked at sub-ambient temperatures. As the crosslink temperature is increased beyond T_c, however, G' monotonically decreases (by a factor of nearly 80 at 64°C). This reduction is due to the spatial heterogeneity of the crosslinked HPC molecular network. Nonporous hydrogels, for instance, consist of a molecular network that uniformly spans the entire specimen analyzed, whereas the HPC network resides almost exclusively within the struts of microporous hydrogels. Included for the sake of comparison

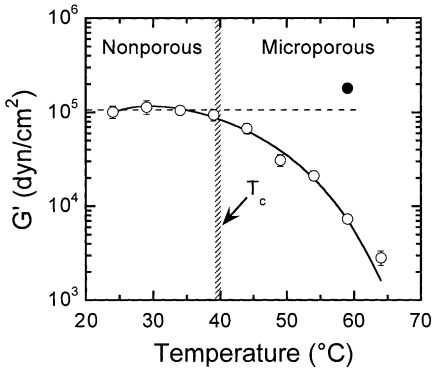

Fig. 7. Dependence of G' (at low ω) on crosslink temperature for 14 wt% HPC hydrogels crosslinked for 5.0 min (○) and 24 h (●). Note that G' remains relatively temperature-invariant below the cloud point (T_c = 39–40°C, from spectrophotometry), but decreases monotonically with increasing temperature above T_c for hydrogels with $t_x = 5.0$ min. The solid line serves as a guide for the eye.

in Fig. 7 are values of G' measured for nonporous and microporous hydrogels crosslinked for 24 h at 34 and 59°C, respectively. The indistinguishable change in G' at 34°C suggests that the HPC network is fully crosslinked under both sets of experimental conditions examined (i.e. $t_x = 5.0$ min at 34°C and $t_a = 24$ h at 24°C versus $t_x = 24$ h at 34°C). In marked contrast, the substantial increase in G' due to extended crosslinking at 59°C indicates that the bulk properties of microporous HPC hydrogels are more sensitive to t_x than their nonporous analogs of identical composition.

Determination of the crosslink efficiency (η) requires both the effective crosslink density (ρ_x) and the theoretical crosslink density (ρ_t), since

$$\eta \equiv \frac{\rho_x}{\rho_t} \tag{1}$$

The value of ρ_t depends on the crosslinking agent employed and is given by [23–25]

$$\rho_t = cf/2 \tag{2}$$

where c and f are the concentration and functionality, respectively, of the crosslinking agent. For DVS, f is determined [26] to be 4. The effective crosslink density is given by

$$\rho_x = \frac{G}{\phi^{4/3}RT} \tag{3}$$

where G is the plateau shear modulus, ϕ is the volume fraction of polymer, R is the universal gas constant and T denotes absolute temperature. Under the conditions where $G'(\omega) \gg G''(\omega)$ and G' is independent of ω (see, for example, Figs. 4 and 6), G can be equated to G'. The volume fraction of HPC can be estimated from the equilibrium swelling ratio (q), which provides a general measure of the amount of liquid that a gel matrix can absorb (or expel) as it swells (or contracts) and which is defined by [24]

$$q \equiv \frac{m_{swollen}}{m_{dry}} \tag{4}$$

where m represents mass. Since q is based on mass, rather than volume, it is related to ϕ through the following:

$$\phi = [1 + (q - 1)\, d_p/d_w]^{-1} \tag{5}$$

Here, d_i (i = p or w) is the mass density of species i: 1.17 g/cm^3 for polymer (p) and 1.00 g/cm^3 for water (w).

Before addressing the effect of crosslink temperature on ρ_x, it is first necessary to examine the temperature dependence of q, which is displayed for HPC hydrogels crosslinked for 5.0 min and 24 h in Fig. 8. Over a broad temperature range that slightly exceeds T_c, q is virtually invariant with respect to temperature and averages about 15.5. This behavior is consistent with the temperature independence of G' seen in Figs. 5 and 7 over a comparable temperature range. One apparent difference in these properties is that G' gradually begins to decrease at T_c, whereas q

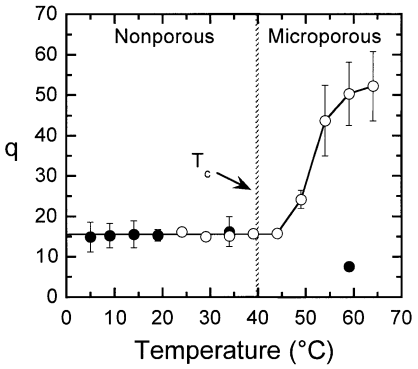

Fig. 8. Equilibrium swelling degree (q) of 14 wt% HPC hydrogels provided as a function of crosslink temperature for crosslink times of 5.0 min (○) and 24 h (●). The solid line serves as a guide for the eye, and the error bars denote one standard deviation in the data.

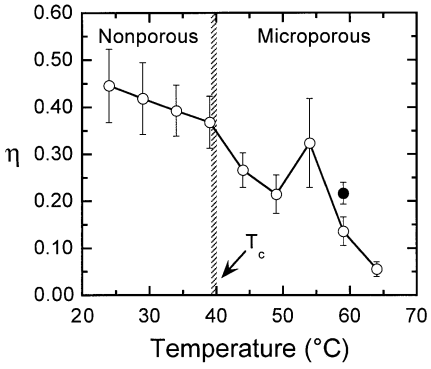

Fig. 10. Dependence of the crosslink efficiency (η) on initial crosslink temperature for 14 wt% HPC hydrogels crosslinked for 5.0 min (○) and 24 h (●) at temperatures above ambient. The solid line connects the data corresponding to hydrogels with $t_x = 5.0$ min.

undergoes an abrupt increase a few degrees above T_c. This increase in q with respect to temperature is most pronounced between 50 and 55°C, but becomes more gradual at higher temperatures, possibly suggesting the existence of a plateau. Swelling ratios obtained from the two HPC hydrogels crosslinked for 24 h at elevated temperatures (see Fig. 7) are also included in Fig. 8. The value of q corresponding to the nonporous hydrogel is similar to that of the hydrogel crosslinked for only 5.0 min at 34°C (recall that their dynamic storage moduli are identical). In the case of the microporous hydrogel synthesized at 59°C, though, q evaluated at $t_x =$ 24 h is just under 8, whereas q at $t_x = 5.0$ min is about 50. Thus, it follows that the enhanced rigidity of this microporous hydrogel (evidenced by the significant increase in G' in Fig. 7) nearly neutralizes its responsiveness (i.e. its ability to undergo a substantial volumetric change).

Substitution of the values of q provided in Fig. 8 into Eq. (5), accompanied by the data presented in Figs. 5 and 7, yields the temperature-dependent ρ_x values shown in Fig. 9. The large error bars on the data collected at subambient temperatures reflect the specimen variability discussed earlier with respect to Fig. 5 and preclude further analysis of these data. Generally speaking, the ρ_x corresponding to HPC hydrogels crosslinked for 5.0 min exhibit a gradual reduction with increasing temperature, which becomes more pronounced at temperatures above T_c. The one obvious exception to this trend occurs at 54°C. We attribute this local maximum to the abrupt and dramatic change in q at this temperature (see Fig. 8). An unexpected result included in Fig. 9 is the value of ρ_x deduced for the microporous hydrogel crosslinked for 24 h at 59°C. Although its bulk properties (G' and q) differ markedly from those of its counterpart crosslinked for only 5.0 min, its ρ_x is not very different from those of the hydrogels crosslinked at comparable temperatures for 5.0 min. Values of the crosslink efficiency (η) derived from Eq. (1) are shown in Fig. 10 for HPC hydrogels crosslinked at ambient and elevated temperatures. With the exception of η discerned at 54°C, a monotonic reduction in η with increasing crosslink temperature is again evident in this figure (from about 45 to 5% over the temperature range examined). This reduction becomes more pronounced at temperatures above T_c and is attributed to confinement of most of the HPC chains to the localized environment (e.g. struts) of the polymer-rich phase during microporous gel formation.

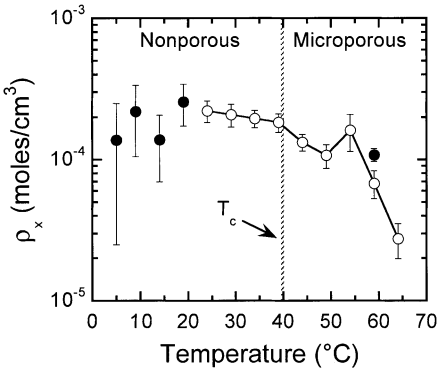

Fig. 9. Effective crosslink density (ρ_x) of 14 wt% HPC hydrogels presented as a function of crosslink temperature for crosslink times of 5.0 min (○) and 24 h (●). Values of ρ_x are determined from Eq. (3) in the text. The solid line connects the data corresponding to hydrogels with $t_x = 5.0$ min.

4. Conclusions

Hydrogels derived from LCST cellulose ethers, such as HPC, can be prepared as either nonporous or microporous, depending on the conditions under which crosslinking occurs. In nonporous hydrogels prepared at temperatures below the cloud point of aqueous HPC, the crosslinked molecular network generally extends uniformly throughout the entire specimen, thereby endowing the resultant material with bulk properties that are not very temperature-dependent. At low temperatures approaching the freezing point of water, however, crosslinking becomes less uniform, resulting in

position-dependent property variation within specimens. If aqueous HPC solutions are crosslinked (even for relatively short times, such as 5.0 min) at temperatures above their cloud point, phase separation is sufficiently rapid to induce a microporous hydrogel morphology that possesses a reduced shear modulus, but greater swelling capacity, than its nonporous analog of identical HPC composition. In this case, the crosslinked HPC network resides predominantly in the polymer-rich phase, that is, in the struts that comprise the bulk morphology. While the modulus of microporous HPC hydrogels may be improved through the use of longer crosslink times, the material effectively loses its swelling capacity upon doing so. The results provided herein confirm that the HPC hydrogel morphology, which can be tailored through judicious combination of crosslink time and temperature in the modified TIPS method, [15] has a significant impact on the bulk properties that make hydrogels so fundamentally interesting and technologically important. Additional environmental considerations such as solution pH, as well as molecular factors such as degree of substitution, molecular weight and polydispersity [27], can influence the phase behavior of aqueous HPC and are expected to have noticeable effects on the properties of hydrogels derived from HPC.

Acknowledgements

We are indebted to Prof. S.H. Gehrke (Kansas State University) for valuable advice and provision of the hydrogel displayed in Figs. 1–3. S.G.H. also thanks Profs. N.S. Allen and S.A. Khan, as well as Ms. E.A. Wilder and Ms. T.A. Walker, for technical assistance and the Environmental Protection Agency for partial financial support.

References

[1] Werbowyj RS, Gray DG. Macromolecules 1980;13:69.
[2] Fortin S, Charlet G. Macromolecules 1989;22:2286.
[3] Spontak RJ, El-Nokaly MA, Bartolo RG, Burns JL. In: Noda I, Rubingh DN, editors. Polymer solutions, blends, and interfaces. Amsterdam: Elsevier Scientific, 1992. p. 273–98.
[4] Fischer H, Murray M, Keller A, Odell J, A. J Mater Sci 1995;30:4623.
[5] Guido S. Macromolecules 1995;28:4530.
[6] Kabra BG, Gehrke SH. ACS Symp Ser 1994;573:76.
[7] Harsh DC, Gehrke SH. J Control Rel 1991;17:175.
[8] O'Connor SM, Gehrke SH. J Appl Polym Sci 1997;66:1279.
[9] Gehrke SH. Adv Polym Sci 1993;110:81.
[10] Harsh DC, Gehrke SH. ACS Symp Ser 1993;520:105.
[11] Ottenbrite RM, Huang SJ, Park K, editors. ACS Symp Ser 1996;627.
[12] Okano T, editor. Biorelated polymers and gels: controlled release and applications in biomedical engineering. New York: Academic Press, 1998.
[13] Buchholz F, Graham A, editors. Modern superabsorbent polymer technology. New York: Wiley, 1998.
[14] Alvarez-Lorenzo C, Gomez-Amoza JL, Martinez-Pacheco R, Souto C, Concheiro A. Int J Pharm 1999;180:91.
[15] Kabra BG, Gehrke SH, Spontak RJ. Macromolecules 1998;31:2166.
[16] Frey MW, Cuculo JA, Spontak RJ. J Polym Sci B: Polym Phys 1996; 34:2049.
[17] Kabra BG, Akhtar MK, Gehrke SH. Polymer 1992;33:990.
[18] Wu XS, Hoffman AS, Yager P. J Polym Sci, Polym Chem Ed 1992; 30:2121.
[19] Hirokawa Y, Jinnai H, Nishikawa Y, Okamoto T, Hashimoto T. Macromolecules 1990;32:7093.
[20] Gao J, Haidar G, Lu XH, Hu ZB. Macromolecules 2001;34:2242.
[21] Winter HH, Chambon F. J Rheol 1986;30:367.
[22] Kavanagh GM, Ross-Murphy SB. Prog Polym Sci 1998;23:533.
[23] Brannon-Peppas L, Harland RS, editors. Absorbent polymer technology. Amsterdam: Elsevier, 1990.
[24] O'Connor SM, Gehrke SH. J Appl Polym Sci 1997;66:1279.
[25] Gehrke SH, Palasis M, Akhtar K. Polym Int 1992;29:29.
[26] Anbergen U, Oppermann W. Polymer 1990;31:1854.
[27] Wang BC, Spontak RJ. Liq Cryst 1997;22:359.